Geographic Routing in Duty-Cycled Industrial Wireless Sensor Networks With Radio Irregularity

LEI SHU[1,2], (Senior Member, IEEE), MITHUN MUKHERJEE[1], (Member, IEEE), LIKUN HU[1,3], NEIL BERGMANN[4], (Member, IEEE), AND CHUNSHENG ZHU[5], (Member, IEEE)

[1]Guangdong Provincial Key Laboratory of Petrochemical Equipment Fault Diagnosis, Guangdong University of Petrochemical Technology, Maoming 525000, China
[2]Lincoln, Lincolnshire, LN6 7TS, United Kingdom
[3]College of Information and Computer Engineering, Northeast Forestry University, Harbin 150040, China
[4]School of Information Technology and Electrical Engineering The University of Queensland, Brisbane, QLD 4072, Australia
[5]Department of Electrical and Computer Engineering, The University of British Columbia, Vancouver, BC V6T 1Z4, Canada

Corresponding author: M. Mukherjee (mithun.mukherjee@outlook.com)

ABSTRACT Industrial wireless sensor networks (IWSNs) are required to provide highly reliable and real-time transmission. Moreover, for connected K-neighborhood (CKN) sleep scheduling-based duty-cycled IWSNs in which the network lifetime of IWSNs can be prolonged, the two-phase geographic greedy forwarding (TPGF) geographic routing algorithm has attracted attention due to its unique transmission features: multi path, shortest path, and hole bypassing. However, the performance of TPGF in CKN-based duty-cycled IWSNs with radio irregularity is not well investigated in the literature. In this paper, we first evaluate the impact of radio irregularity on CKN-based duty-cycled IWSNs. Furthermore, we investigate the routing performance of TPGF in CKN-based duty-cycled IWSNs with radio irregularity, in terms of the number of explored routing paths as well as the lengths of the average and shortest routing paths. Particularly, we establish the upper bound on the number of explored routing paths. The upper bound is slightly relaxed with radio irregularity compared with without radio irregularity; however, it is bounded by the number of average 1-hop neighbors in always-on IWSNs. With extensive simulations, we observe that the cross-layer optimized version of TPGF (i.e., TPFGPlus) finds reliable transmission paths with low end-to-end delay, even in CKN-based duty-cycled IWSNs with radio irregularity.

INDEX TERMS Industrial Wireless Sensor Networks, Sleep Scheduling, Geographic Routing, Radio Irregularity.

I. INTRODUCTION

*I*ndustrial Wireless Sensor Networks (IWSNs): Recently, due to advantages such as low cost, ease-of-deployment, energy efficiency, and mobility compared to the traditional wired field-bus, Industrial Wireless Sensor Networks (IWSNs) have become a promising approach [1] in many industrial applications, e.g., robotics, large-scale pipeline and equipment monitoring, fault diagnosis and toxic gas detection.

Compared to traditional WSNs, IWSNs have the following unique characteristics

- As well as cross-technology *interference* due to coexisting wireless devices, IWSNs suffer from harsh environments, with rotation, friction, vibration, noise, humidity, temperature fluctuations and the like.

- Moreover, IWSNs suffer more seriously from the *limited* lifetime problem compared to traditional WSNs because of limited sensor size, difficult access (e.g., heat exchange tube and rotating machines), and limited energy harvesting possibilities.
- In addition, *reliable* and *real-time* transmission are essential to guarantee effective industrial control.

*G*eographic Routing in Duty-cycled IWSNs: Highway Addressable Remote Transducer protocol (HART) is a common industrial networking protocol. Although the well-known HART-based wireless standard, WirelessHART, supports reliable and low latency transmission in various applications, it is not scalable. The complexity of routing algorithms must be scalable, i.e., be independent from the size of the network as the number of sensor nodes ranges

TABLE 1. Comparison of various geographic routing schemes.

Protocols	Routing strategies	Drawback	Radio Irregularity
GeRaF [2]	Geographic random forwarding	Does not consider duty-cycled WSNs	×
TGF [3]	Marcov-decision-based greedy routing	Does not consider duty-cycled WSNs	×
McTPGF [4]	Considers multimedia networks, focuses on low end-to-end delay	Energy consumption is not considered.	×
EBGR [5]	Energy-efficient beaconless geographic routing protocol and considers high variant link quality	Does not consider residual energy for making forwarding decision	Considered, however with disc-shaped model
GPSR [6]	Hole bypassing greedy forwarding, uses planarization algorithms	Local minimum problem and maintenance of underlying planar graph	×
TPGF [7]	Explores the possible number of routing path using shortest path criteria, hole bypassing and avoids local minimum	Does not consider duty-cycled WSNs	×
TPFGPlus [8]	Energy-balanced sleep scheduling scheme with cross-layer optimized geographic node-disjoint multipath routing algorithm	Does not consider radio irregularity	×
GSS [9]	Decreases the length of first transmission path searched by TPGF	Does not consider link asymmetry	×
GCKNF [10]	Minimizes the length of first transmission path explored by geographic routing in duty-cycled mobile WSNs	Does not consider link asymmetry	×
GCKNA [10]	Reduces the length of all paths searched by geographic routing in duty-cycled mobile WSNs	Does not consider link asymmetry	×

from tens to thousands. Geographic routing has emerged as a promising approach due to its simplicity, scalability, and efficiency regardless of the network size. Geographic routing in *duty-cycled* IWSNs is a new approach in which a node forwards packets only to its 1-hop *awake* neighbors that are geographically closer to the sink, while other neighbors are allowed to sleep to save the energy. At present, most of the sleep scheduling algorithms in duty-cycled IWSNs focus on either global connectivity or coverage issues. A connected *k*-neighborhood (CKN) [11]-based sleep scheduling approach[1] is widely used because this algorithm efficiently allows the network to be *k*-connected with a minimum number of awake nodes, therefore prolonging the network lifetime.

Many opportunistic routing algorithms [2], [6], [12]–[15] have been proposed for duty-cycled WSNs, however, the local minima and hole problems still exist in these algorithms. The two-phase geographic greedy forwarding (TPGF)[2] algorithm [7] has drawn significant attention because 1) it can overcome these above-mentioned problems with multi-path transmission, hole-bypassing without prior hole information, and shortest path transmission characteristics, and 2) TPGF facilitates data streaming in always-on WSNs [16] and focuses on exploring the maximum number of optimal node-disjoint routing paths to minimize the path length and the end-to-end transmission delay. A modified cross-layer optimized geographic routing called TPFGPlus [8] balances the energy consumption in the duty-cycled WSNs with environmental energy harvesting. In [9], the main aim of the Geographic routing-oriented Sleep Scheduling (GSS) is to decrease the length of the first transmission path searched by TPGF. A comparative study on geographic routing in duty-cycled WSNs is summarized in Table I.

[1]CKN algorithm has the following characteristics: 1) each node have at least $\min(N_u, k)$ awake neighbors in each epoch, where N_u is the set of 1-hop neighbors of node *u* and *k* is any positive integer, 2) all awake nodes will be connected, 3) every node (awake or asleep) has an awake neighbor, and 4) the set of awake nodes changes from epoch to epoch.

[2]In first phase of TPGF, the chosen neighbor node must be nearer to the sink than the node itself. If the node does not find any forwarding neighbor node, then it steps back to its previous-hop node with an attempt to explore a path to the sink. This overcomes the local minima problem. The second phase optimizes the path by deleting unnecessary nodes.

*R*adio Irregularity: Unlike a perfect circular reception area model in traditional WSNs, a high variation in packet-error-ratio (PER) is observed in the transitional region [17]–[21]. Path loss, cross-technology interference, and the non-isotropic nature of the electromagnetic (EM) transmission [21], [22] are mainly responsible for radio irregularity in low-powered IWSNs. Other factors, e.g., temperature, weather, and equipment noise also influence the received signal power. The impact of irregularity on the message reception probability was investigated in [23]. It is found that this irregularity phenomena are not always correlated with distance, however, strongly depend on the radio characteristics of a link [18], [20].

A. MOTIVATION
Although the TPGF-based routing algorithms provide a good trade-off between end-to-end transmission delay, reliability, and energy efficiency in duty-cycled IWSNs, none of them [4], [7]–[10], [12], [16] consider the effect of radio irregularity in the system model. Furthermore, it is observed in [19] that more nodes need to be awake in duty-cycled IWSNs to satisfy the required *k*-connectivity when there is a higher number of irregular nodes as well as link asymmetry. Fig. 1 illustrates an example of CKN-based sleep scheduling schemes with various percentages of irregular nodes and different levels of link asymmetry. The adverse impact of radio irregularity on the number of awake nodes is observed. Since radio irregularity normally exists in harsh industrial environments, its impact cannot be ignored in the routing schemes with duty-cycled IWSNs. This motivates us to evaluate the effect of radio irregularity on geographic routing in duty-cycled IWSNs.

B. CONTRIBUTION
The main contributions of this paper are summarized as follows.
- To investigate the number of paths explored by TPGF-based geographic routing algorithms in

[3]NetTopo (online at http://sourceforge.net/projects/nettopo/) is an open source software for simulating and visualizing WSNs.
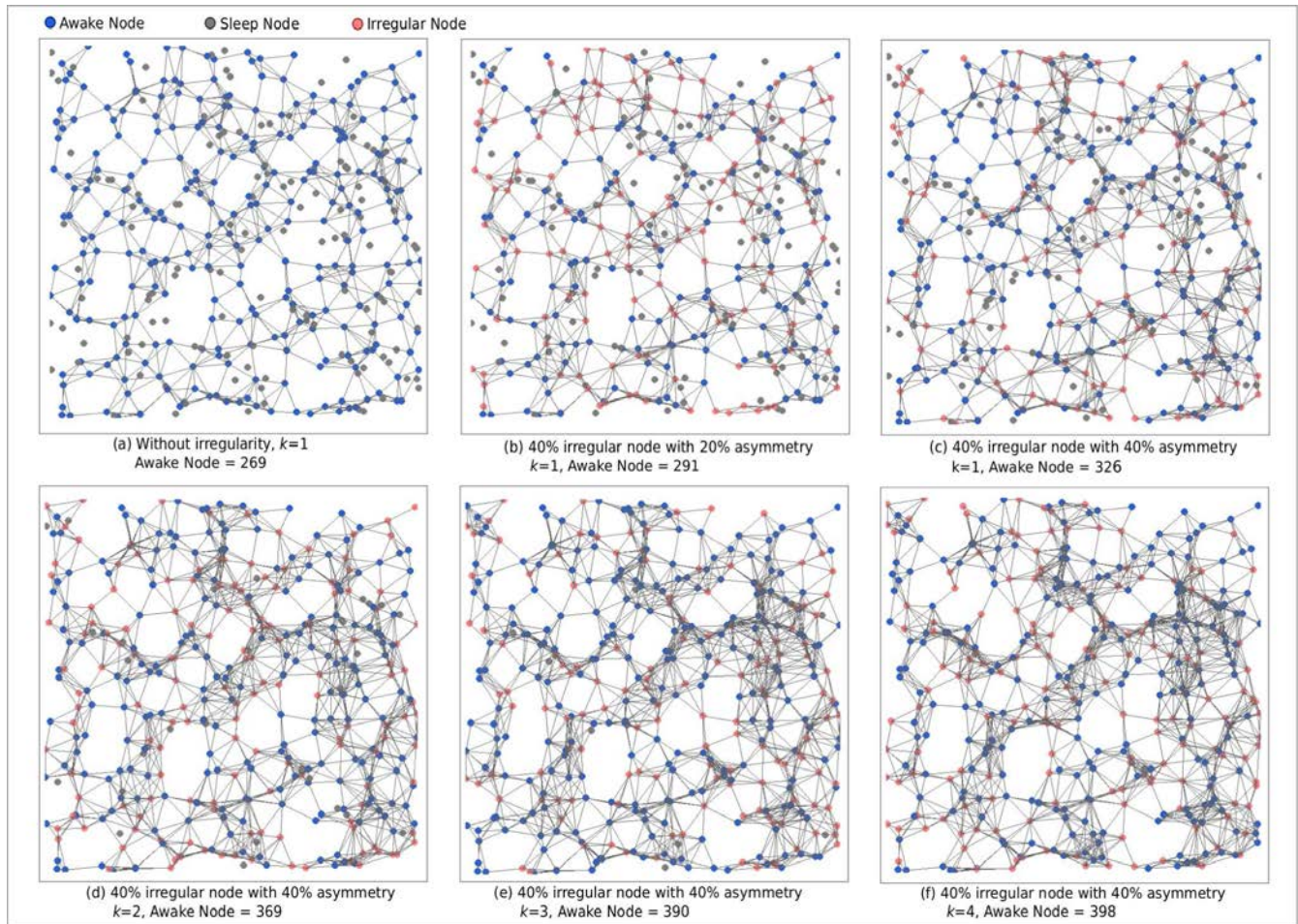
FIGURE 1. Impact of radio irregularity on awake node in the CKN-based sleep scheduling with a network size 600×600 m^2 and $N = 400$ deployed nodes. We use a WSN simulator NetTopo.[3] (a) Without link asymmetry, (b)-(c) The number of awake node is increased to 40% link asymmetry compared with 20% link asymmetry with same number of irregular nodes. (d)-(f) Moreover, the number of awake node increases to maintain higher k-connectivity in presence of link asymmetry with irregular nodes. Almost all the sensor nodes are always-on with high k-value, i.e., $k = 4$.

duty-cycled IWSNs with radio irregularity, we first evaluate the impact of radio irregularity on duty-cycled IWSNs. We further study the performance of geographic routing in duty-cycled IWSNs with radio irregularity.

- We analytically establish the upper bound on the number of explored routing paths by using TPGF with CKN-based IWSNs. Extensive simulation results are provided on the number of explored paths, average, and shortest path lengths for TPGF-based routing algorithms with radio irregularity.

The rest of the paper is organized as follows. Section II presents the system model. The upper bound on the maximum number of explored paths for TPGF with CKN in the presence of radio irregularity is studied in Section III. The simulation results are presented in Section IV. Finally, conclusions are drawn in Section V.

II. SYSTEM MODEL

*N*etwork Model: We consider a multihop IWSN with uniformly and randomly deployed sensor nodes in a large-scale 2-dimensional industrial sensing field. Let $G = (U, L)$ be a network graph, where $U = \{u_1, u_2, \ldots u_N\}$ and $L = \{l(1, 2), l(1, 3), \ldots, l(N - 1, N)\}$ are the set of N sensor nodes and the set of edges between sensor nodes, respectively. Two sensor nodes $\{u, v\} \in U$ are called 1-hop neighbors if they are within the transmission range of each other and $l(u, v) \in L$. We assume bi-directional communications between 1-hop neighbors. We use the well-known Request-To-Send (RTS)/Clear-To-Send (CTS)-based link scheduling [10] to prevent message collisions. The location of any sensor node along with its 1-hop neighbors can be obtained by using the Global Positioning System (GPS) or other localization techniques. The sink node knows the location and IDs of all nodes. It is also assumed that each node has the same functionality and sensing capability. A dense network is assumed in our model. The main notations in this paper are summarized in Table II.

*R*adio Irregularity Model: We consider the Radio Irregularity Model (RIM) in [17]. Assume that each node u loses its unidirectional link $\text{link}_{u \to v}$ to any node v $\forall v \in N_u$ with

TABLE 2. Main notation definition.

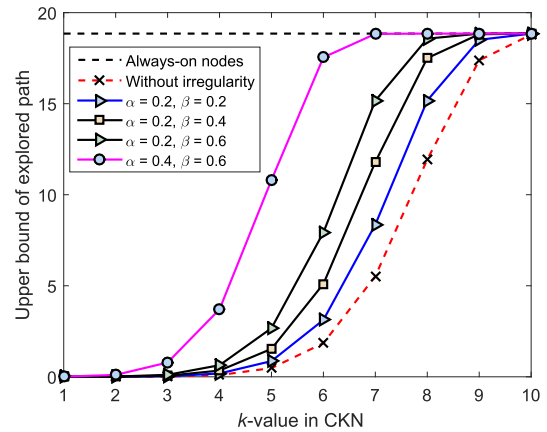| Symbols	Definition
$\lvert \cdot \rvert$	The number of elements in a set
N	The number of total sensor nodes in the network
U	The set of sensor nodes in the network
L	The set of links
$l(u,v)$	The bi-directional link between u and v nodes, $\{u,v\} \in U$
r	Ideal transmission range without radio irregularity
$\mathcal{A}$	The area of the network
ρ	The node density in the network
$\alpha(u)$	The probability of losing neighbor of the uth node due to radio irregularity
β	The probability that how many nodes have the link asymmetry problem
rank_u	The random rank picked by the uth node
N_u	The set of the uth 1-hop neighbor
N_u'	The set of the uth 2-hop neighbor
$C_u, C_u',$ and U'	The subset of $N_u, N_u',$ and U whose ranks $\leqslant \mathrm{rank}_u$
λ	The input packet rate of the uth node
γ	The output packet rate of the uth node
T	The time to run the sleep scheduling algorithm
N_{Epoch}	The number of epoch in lifetime of the network
E_0	The initial energy of the sensor node
E_{amp}	The energy consumed in the amplifier of transmitter to send a packet at unit distance
E_{elec}	The energy consumed in the transceiver circuitry

FIGURE 2. Analytical plot of upper bound on the explored path in the TPGF-based routing with irregular nodes, link asymmetry, and different *k*-value in the CKN-based sleep scheduling with *N* = 600 nodes.

a probability $\alpha(u)$ at each instant due to the time-varying nature of radio irregularity. Since we assume RTS/CTS-based link scheduling, the quality of the bi-directional link $l(u,v)$ strongly depends on $\alpha(u)$ and $\alpha(v)$ $\forall v \in N_u$. Let β be the ratio of the number of nodes with link asymmetry problems and the total number of deployed nodes in a given area $\mathcal{A}$. We observe that the success rate of a bi-directional link depends on individual nodes losing connection, i.e., $\alpha(u)$ as well as number of nodes that suffer from link asymmetry, which is related to β. Without loss of generality, we denote $\alpha(u)$ and β as link asymmetry and node asymmetry, respectively. For the sake of simplicity, we drop u from $\alpha(u)$ in the rest of the paper.

III. UPPER-BOUND ON THE NUMBER OF EXPLORED PATHS FOR TPGF-BASED ROUTING WITH RADIO Irregularity

The probability that the graph G is k-connected is

$$P(G)_{\text{k-connected}} = \left(1 - \sum_{n=0}^{k-1} \frac{(\rho \pi r^2)^n}{n!} \exp\left(-\rho \pi r^2\right) \right)^N. \quad (1)$$

Similarly, we deduce the probability that the graph $G_{C_u+C_u'}$ is connected as follows

$$\mathrm{Prob}_1 = P\left(G_{C_u+C_u'}\right)_{\text{1-connected}}$$
$$= \left(1 - \exp\left(-\rho' \pi r^2\right) \right)^{(\lvert C_u \rvert + \lvert C_u' \rvert)}, \quad (2)$$

where $\rho' = \lvert U' \rvert / \mathcal{A}$. Therefore, the probability that the graph G_{N_u} is k-connected in C_u is expressed as

$$\mathrm{Prob}_2 = P\left(G_{N_u \sim C_u}\right)_{\text{k-connected}}$$
$$= \left(1 - \sum_{n=0}^{k-1} \frac{(\rho' \pi r^2)^n}{n!} \exp\left(-\rho' \pi r^2\right) \right)^{\lvert C_u \rvert}. \quad (3)$$

Therefore, the sleep probability of the node u in CKN-based sleep scheduling is expressed as $P_{\mathrm{sleep}}(u) = \mathrm{Prob}_1 \times \mathrm{Prob}_2$,

where Prob_1 and Prob_1 consider the two conditions of the CKN algorithm as 1) the graph $G_{C_u+C_u'}$ is connected and 2) the graph G_{N_u} is connected by C_u nodes, respectively.
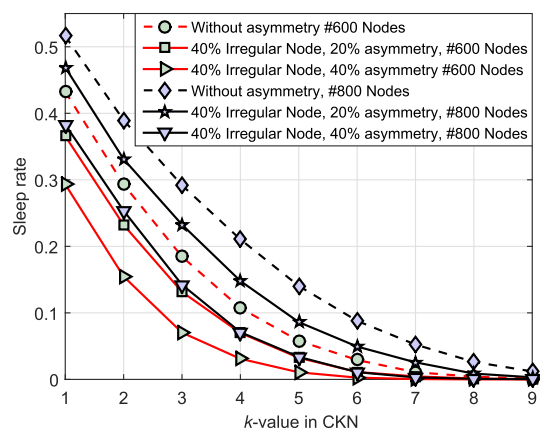

FIGURE 3. Sleep rate with various irregularity parameters with different *k*-value in the CKN-based sleep scheduling with 600 and 800 nodes.

Lemma 1: Since any node forwards its packet to awake 1-hop neighbors, thus the upper bound strongly depends on the k-value in the CKN-based sleep scheduling. More specifically, the maximum number of explored paths for TPGF with CKN-based sleep scheduling is tightly upper-bounded by the awake rate of nodes, i.e., $1 - P_{\mathrm{sleep}}(u)$.

Theorem 1: The upper-bound on number of explored paths is slightly relaxed in the presence of radio irregularity compared to the upper-bound without radio irregularity, however, is always bounded by $\mathbb{E}\left[\lvert N_u \rvert\right] = \rho \pi r^2$ in always-on WSNs.

Proof: Assuming a uniformly and randomly distributed WSN with N nodes in an area $\mathcal{A}$, the probability that any irregular node u has n neighbors with an asymmetry link
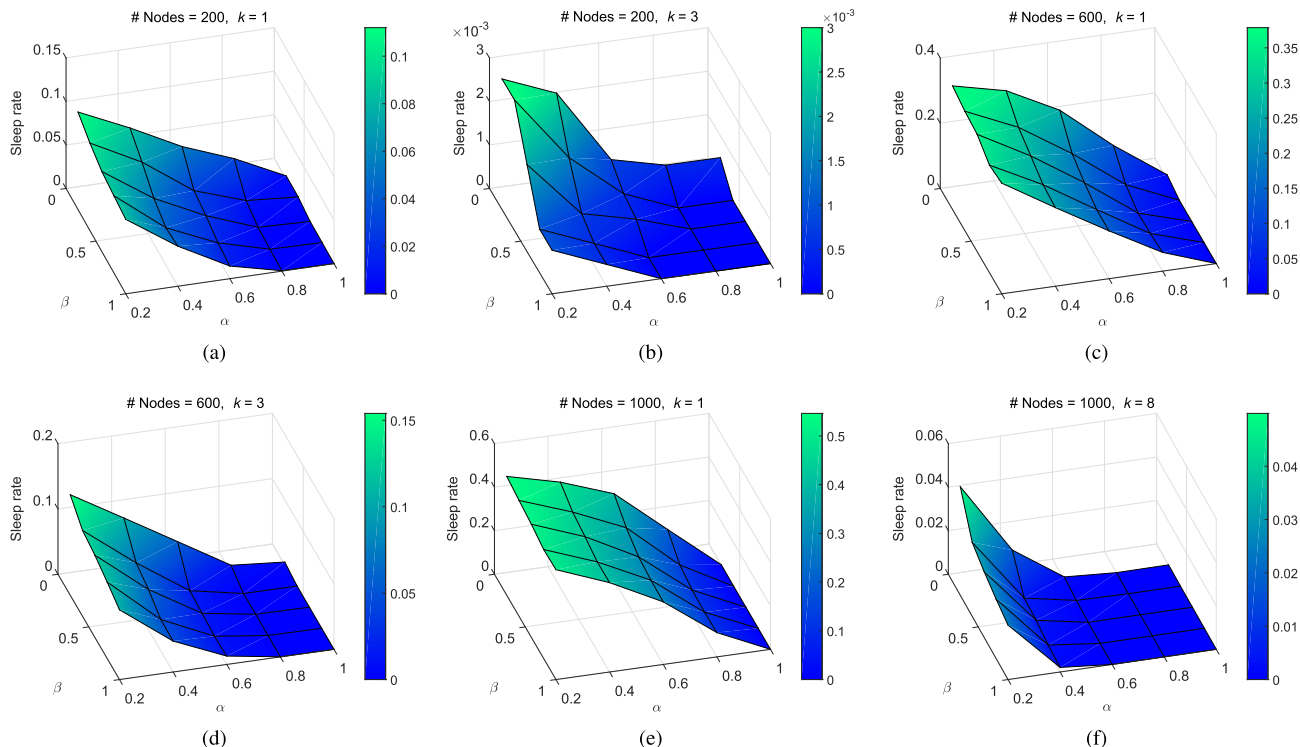
FIGURE 4. Sleep rate with probability of asymmetric node and different link asymmetry at various numbers of deployed nodes with *k* value in *k*-connected CKN-based sleep scheduling.
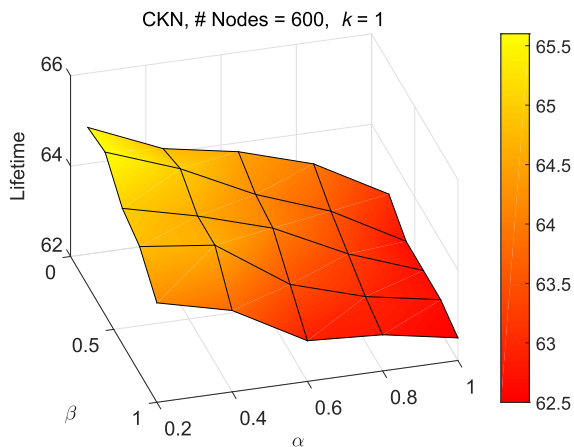

FIGURE 5. Lifetime with probability of asymmetric node and different link asymmetry in CKN-based sleep scheduling.

probability α is given as

$$
\begin{aligned}
&P(|N_u| = n)^{\text{irregular}} \\
&= \frac{\left(\beta(1-\alpha)\rho\pi r^2 + (1-\beta)\rho\pi r^2\right)^n}{n!} \\
&\quad \times \exp\left(-\beta(1-\alpha)\rho\pi r^2 - (1-\beta)\rho\pi r^2\right) \\
&= \frac{\left((1-\beta\alpha)\rho\pi r^2\right)^n}{n!} \\
&\quad \times \exp\left(-(1-\beta\alpha)\rho\pi r^2\right).
\end{aligned} \tag{4}
$$

Thus, the probability that the graph G is connected with the radio irregularity variables β and α is given as

$$
\begin{aligned}
P(G)_{\text{k-connected}}^{\text{irregular}} = \Bigg(1 - \sum_{n=0}^{k-1} \frac{\left((1-\beta\alpha)\rho\pi r^2\right)^n}{n!} \\
\times \exp\left(-(1-\beta\alpha)\rho\pi r^2\right) \Bigg)^N .
\end{aligned} \tag{5}
$$

Using (4–6), the the sleep probability of the node u with the link asymmetry becomes

$$
\begin{aligned}
P_{\text{sleep}}(u)^{\text{irregular}} = \left(1 - \exp\left(-(1-\beta\alpha)\rho'\pi r^2\right) \right)^{\left(|C_u| + |C_u'|\right)} \\
\times \Bigg(1 - \sum_{n=0}^{k-1} \frac{\left((1-\beta\alpha)\rho\pi r^2\right)^n}{n!} \\
\times \exp\left(-(1-\beta\alpha)\rho\pi r^2\right) \Bigg)^{|C_u|} .
\end{aligned} \tag{6}
$$

∎

Fig. 2 shows the analytical plot of explored paths in TPGF with CKN-based sleep scheduling. We observe that the number of explored paths in TPGF with CKN-based sleep scheduling with radio irregularity is always bounded by $\mathbb{E}[|N_u|] = \rho\pi r^2$ in all-awake WSNs.

IV. SIMULATION RESULTS
In this section, we evaluate the impact of radio irregularity in IWSNs on 1) sleeping rate and network lifetime of the CKN-based sleep scheduling and 2) number of explored
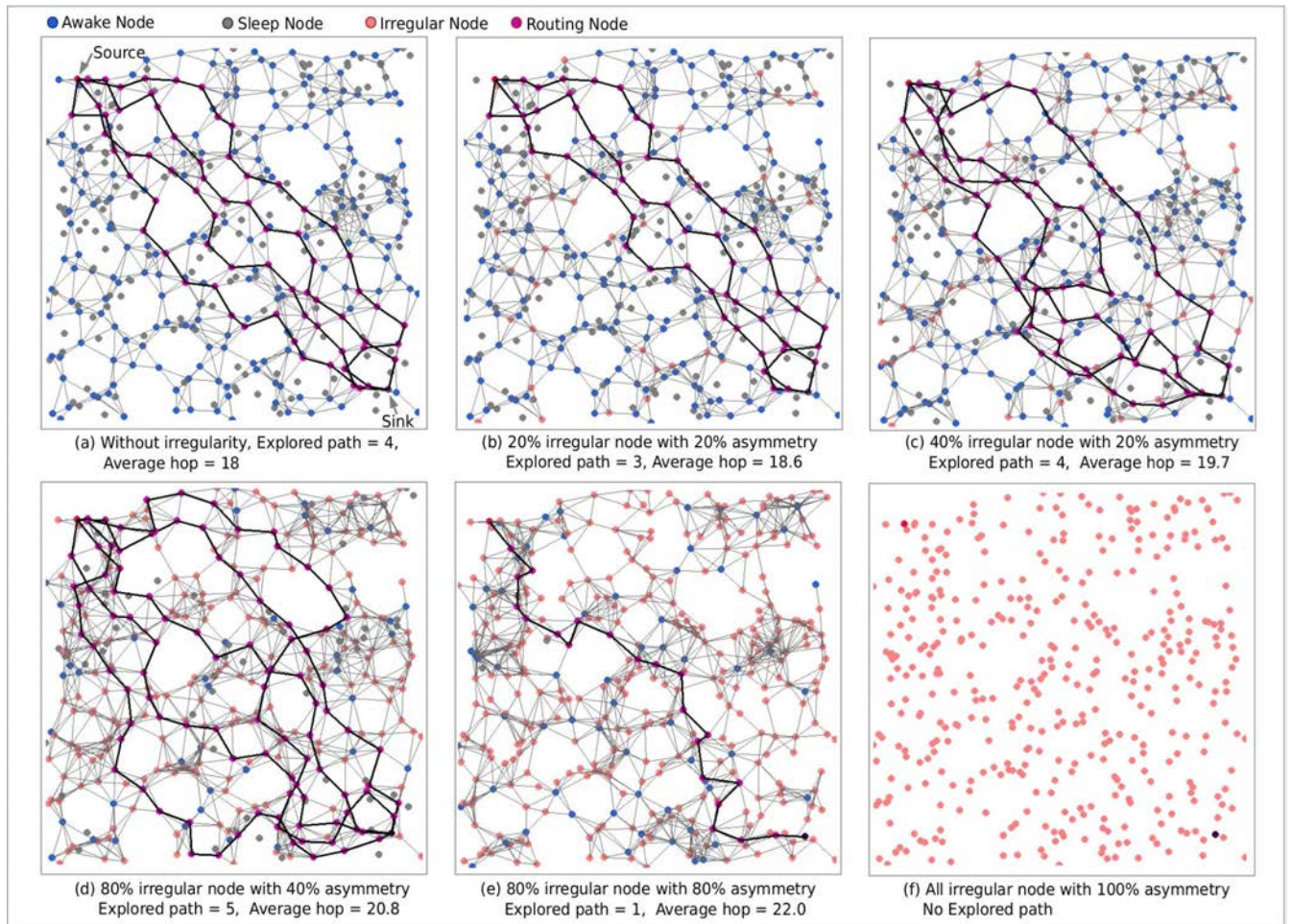
FIGURE 6. The impact of link asymmetry with irregular nodes on the explored paths and average path length in terms of hop-count in CKN-based TPGF algorithms. The network size is 600 × 600 m² with $N = 400$ deployed nodes and $k = 1$. (a)-(e) Number of average hop count increases with the increasing value of link asymmetry compared to without link asymmetry. (f) However, at 100% irregularity with all irregular nodes, no path exists between source to sink.

paths, and average and shortest path length in terms of hop counts in the TPGF-based routing algorithms with the CKN-based sleep scheduling.

*S*imulation setup: We conducted extensive simulations using NetTopo. For each number of deployed sensor nodes, the results are averaged over 100 network topologies. The number of sensor nodes ranges from 200 to 1000 (each time increased by 100). Simulation parameters are summarized in Table III. The network lifetime is defined as the instant from the network deployment to the instant when the first sensor node runs out of energy.

A. PERFORMANCE OF CKN WITH RADIO IRREGULARITY

1) SLEEP RATE VS. K-VALUE WITH DIFFERENT NODE DENSITY

Fig. 3 illustrates the impact of radio irregularity on sleep rate in the CKN-based sleep scheduling algorithms with $\alpha = 0.4$, and $\beta = 0.2$ and 0.4, respectively. The sleep rate degrades with higher k-value since more nodes are awakened to

TABLE 3. Simulation parameters.

Parameters	Values
Network size	600×600 m²
Number of sensor nodes	200 to 1000
k-value in CKN	1 to 10
Transmission radius	60 m
E_{elec}	50 nJ/bit
E_{amp}	50 pJ/bit/m²
Initial energy	100 000 mJ
Time epoch	1 min
Packet size	12 byte
Packet number	1000

satisfy the k-connectivity in the CKN algorithms. The sleep rate is higher in all the cases with 800 node deployment compared to 600 nodes. The reason is that fewer nodes are awakened to maintain the k-connectivity in a higher node deployment. As expected, the sleep rate degrades with the irregularity parameters $\alpha = 0.4$ and $\beta = 0.2$ for both 600 and 800 node deployment. The reason is that *additional* nodes are awakened to maintain the k-connectivity due to the link asymmetry. Furthermore, when the link asymmetry parameter increases from 0.2 to 0.4, the impact is higher
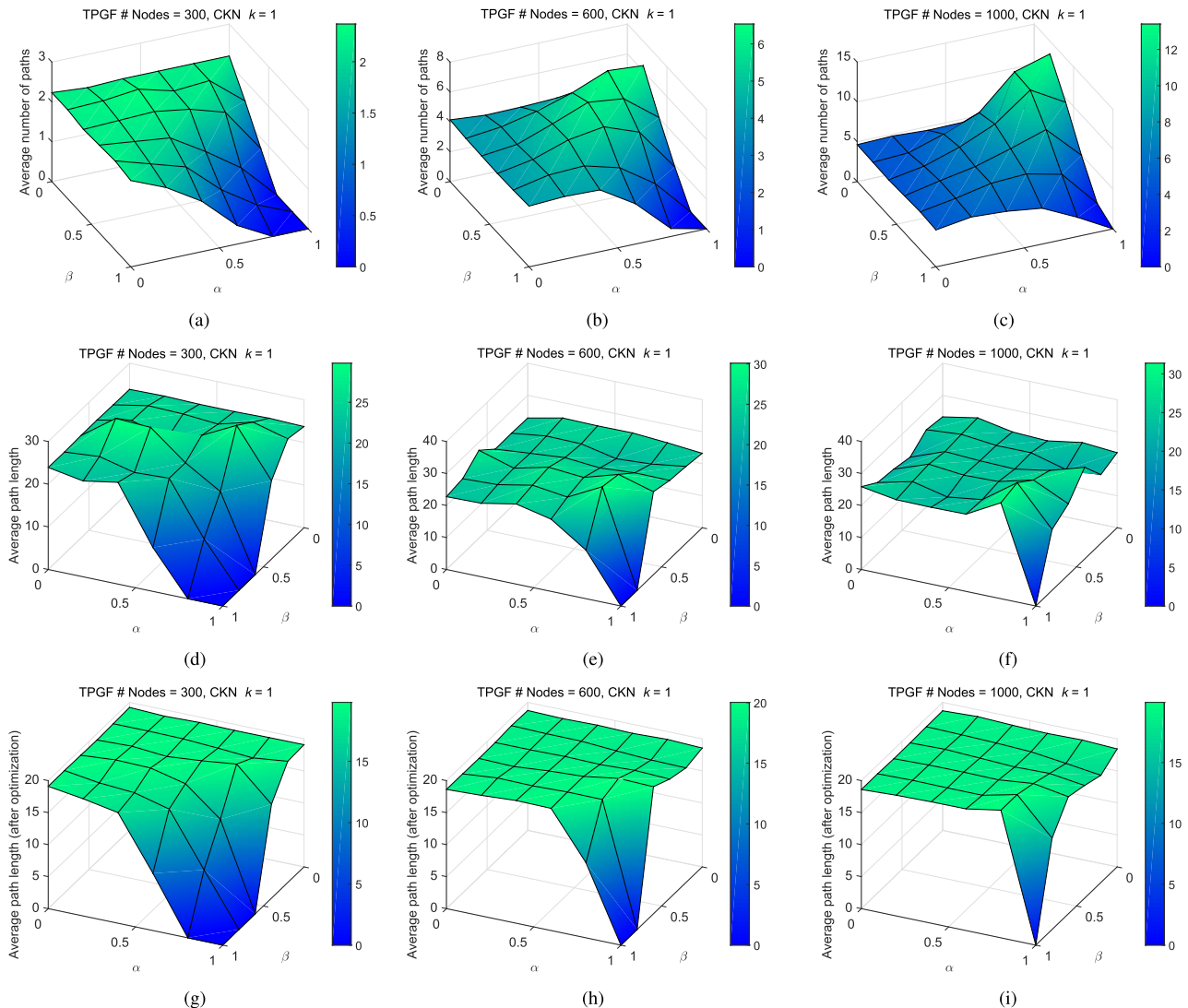
FIGURE 7. Performance of CKN-based TPGF for *k* = 1 with radio irregularity. (a)-(c) Average path number, (d)-(f) Average path length without optimization, and (g)-(i) Average path length after optimization with irregularity parameters *α* and *β*.

compared to the previous value. It is observed that to obtain a sleep rate about 0.07, the maximum *k*-value can be satisfied up to 4 and 3 with {*α* = 0.4 and *β* = 0.2} and {*α* = 0.4 and *β* = 0.4}, respectively with 600 nodes.

2) SLEEP RATE VS. RADIO IRREGULARITY VARIABLES

Next, the impact of varying the parameters *α* and *β* is studied in CKN-based sleep scheduling. From Fig. 4, we observe that the increase of the irregularity parameters results in a large decrease of the sleep rate. As observed in Fig. 4(a), the sleep rate is 0.07 with *α* = 0.4 and *β* = 0.4 with *k* = 1 in 200 node deployment. We see that almost all the nodes are awakened beyond *α* = 0.5 and *β* = 0.6 for *k* = 3. Therefore, the sleep rate tends to zero as shown in Fig. 4(b). Accordingly, from the Fig. 4(c) and Fig. 4(d), we see that the sleep rate is higher in 600 node deployment compared to the previous 200 node deployment due to the larger number of deployed nodes, however, at higher *k*-value, the sleep rate degrades due

to the increasing values of *α*) as well as *β*. The performance of the 1000 node deployment is shown in Fig. 4(e) and Fig. 4(f) with *k* = 1 and *k* = 8, respectively. The sleep rate is higher compared to the previous node density, however, at a higher deployment cost. We also observe that the *k*-connectivity can be maintained up to 8 with *α* = 0.4 and *β* = 0.8 with 1000 nodes. From the results, we confirm that impact of the radio irregularity is increased for higher *k*-values in the CKN algorithm since more deployed nodes are awakened to satisfy the *k*-connectivity constraint.

3) LIFETIME VS. IRREGULARITY PARAMETERS

To see the relationship between lifetime and radio irregularity parameters, we present simulation results in Fig. 5. The network lifetime decreases with the increasing values of radio irregularity parameters *α* and *β*. As the link asymmetry phenomena becomes more serious with more irregular nodes, nodes sleep less and lifetime decreases.
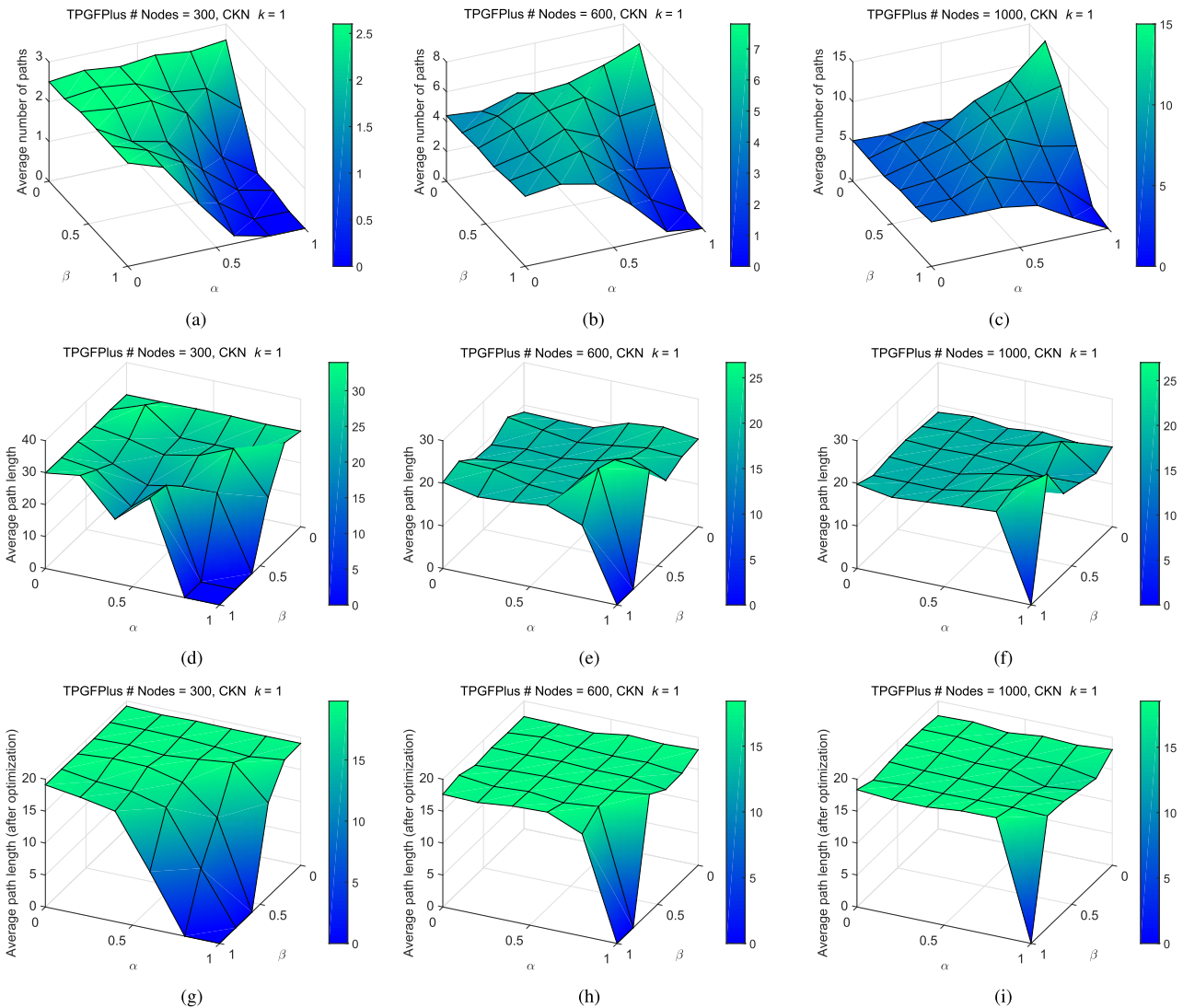
FIGURE 8. Performance of CKN-based TPFGPlus for *k* = 1 with radio irregularity. (a)-(c) Average path number, (d)-(f) Average path length without optimization, and (g)-(i) Average path length after optimization with irregularity parameters *α* and *β*.

B. TPGF AND TPFGPlus WITH RADIO IRREGULARITY

To evaluate the overall performance of TPGF and TPFGPlus, a source and a sink node are deployed at location (50, 50) and (550, 550), respectively.

1) DEMONSTRATION OF EXPLORED PATHS FOR TPGF WITH RADIO IRREGULARITY

The impact of link asymmetry on the explored routing path in a duty-cycled WSN is shown in Fig. 6. The adverse impact on the average length in terms of hop count is observed. As expected, TPGF explores more node-disjoint routing paths when more awake nodes are available because of a small increase in link asymmetry, however at the expense of average hop counts. Finally, as the radio irregularity increases further, the number of explored path reduces. We also note that the TPGF is not able to explore any path when all the nodes are irregular with 100% link asymmetry.

2) AVERAGE NUMBER OF EXPLORED PATHS

Fig. 7 illustrates the performance of TPGF with $k = 1$ in the CKN-based sleep scheduling. Fig. 8(a)–8(c) show the average number of explored paths from the source to the sink with various node density and irregularity parameters. As expected, the number of explored paths increases at higher node density without any link asymmetry i.e., $\alpha = 0$ and $\beta = 0$. From Fig. 8(a), it is observed that as the value of irregularity parameters increases, the explored path number decreases due to link asymmetry with 300 nodes. We recall that the number of awake node increases at higher irregularity parameters α and β to maintain $k = 1$ connectivity in the CKN-based sleep scheduling as shown in Fig. 4(c). Since the explored paths are directly related to the number of awake nodes, the number of explored paths in the TPGF multipath routing with 600 nodes increases beyond α and $\beta \simeq 0.4$ as shown in 8(b). However, few explored paths are found at high

TABLE 4. Performance of TPGF and TPFGPlus with radio irregularity $\alpha = 0.8$ and $\beta = 0.4$.

#Node	k	TPGF			TPFGPlus		
		#Path	Average length	Shortest length	#Path	Average length	Shortest length
300	1	1.88	19.87	18.88	1.51	19.61	18.25
	3	2.00	20.75	19.55	2.00	20.65	18.51
	6	2.33	20.76	19.11	2.53	21.60	18.17
	9	1.12	22.81	22.25	1.12	21.71	20.15
600	1	4.72	18.70	16.11	5.81	19.46	16.01
	3	6.62	22.35	15.13	6.65	21.55	14.13
	6	6.63	27.21	15.14	6.83	28.14	14.56
	9	6.21	23.91	15.12	6.23	22.41	14.72
1000	1	6.51	24.04	16.13	6.10	18.26	16.21
	3	10.9	25.93	14.83	11.2	24.31	14.31
	6	13.3	21.53	14.46	14.7	20.73	14.02
	9	13.3	21.49	14.31	14.3	20.89	13.93

link asymmetry. As can be seen from the Fig. 8(a)-8(c), no path is found from the source to the sink when the values of α and β tend to 1. Similarly, more explored paths are found at about α and $\beta \simeq 0.5$ in 1000 nodes, however, with a deployment cost.

3) AVERAGE PATH LENGTH
Fig. 8(d)–8(f) shows the average path length performance in TPGF. Since the TPGF algorithm explores possible routing paths even in the presence of the radio irregularity, the average path length is about 22-to-24 when asymmetry parameters are about α and $\beta \simeq 0.4$ for all deployments. However, for 300 nodes, in some cases, no routing path from source to sink is found for a given network topology. Therefore, averaging over the different topologies leads to reduced path length as shown in Fig. 8(d). However, from Fig. 8(e) and Fig. 8(f), it is observed that the average path length is better in higher node deployment, i.e., 1000, compared to previous low node deployment, i.e., 600 and 300. With more awake nodes, the routing path still exists even in presence of adverse radio irregularity in higher node deployment. However, when α and β tend to 1, none of the deployments is able to explore any routing path.

4) OPTIMIZED AVERAGE PATH LENGTH
We present the simulation results after optimizing the path found by TPGF as in [7]. From Fig. 8(g)–8(i), it is clear that the optimized path length is more stable than without optimization. In addition, in most of the cases, the path length is below 20 hops compared to without optimization where the average path length is above 20 hops. As a result, the reduced path length provides lower end-to-end delay in presence of radio irregularity.

5) TPGF AND TPFGPlus WITH VARIOUS K-CONNECTIVITY
The performance with various k-values and node densities in CKN-based TPGF is shown in Table IV. When, more nodes are awakened to satisfy high k-connectivity, the number of explored paths increases. Although the reliability is enhanced with more node-disjoint paths in higher k-connectivity graphs, a trade-off among low end-to-end transmission in terms of average length of the path, number of awake node, and the explored path is observed. As expected, TPFGPlus performs significantly better in dense networks and higher k-connectivity in duty-cycled IWSNs. Note that the performance of the shortest path in TPFGPlus is always better than TPGF in all the scenarios.

V. CONCLUSION
This article has studied the performance of TPGF geographic routing in CKN based duty-cycled IWSNs with radio irregularity. The upper bound on the maximum number of explored node-disjoint routing paths has been established. It has been observed that the upper bound is slightly relaxed in the presence of radio irregularity compared to the upper-bound without radio irregularity, however, it is always bounded by the expected number of 1-hop neighbors in always-on IWSNs. Particularly, as the sleep rate decreases when there is higher k-connectivity in CKN based duty-cycled IWSNs with radio irregularity, TPGF explores more node-disjoint routing paths when more awake nodes are available, however at an expense of average hop counts. Furthermore, due to its inherent advantages, TPFGPlus always finds reduced average and shortest path lengths compared to TPGF, therefore, it provides low end-to-end delay for CKN based duty-cycled IWSNs even with radio irregularity.

REFERENCES
[1] K. Xu, Y. Qu, and K. Yang, "A tutorial on the Internet of Things: From a heterogeneous network integration perspective," *IEEE Network*, vol. 30, no. 2, pp. 102–108, Mar. 2016.

[2] M. Zorzi and R. R. Rao, "Geographic random forwarding (GeRaF) for ad hoc and sensor networks: Multihop performance," *IEEE Trans. Mobile Comput.*, vol. 2, no. 4, pp. 337–348, Oct. 2003.

[3] K. P. Naveen and A. Kumar, "Tunable locally-optimal geographical forwarding in wireless sensor networks with sleep-wake cycling nodes," in *Proc. IEEE INFOCOM*, Mar. 2010, pp. 1–9.

[4] K. Wang, L. Wang, C. Ma, L. Shu, and J. J. P. C. Rodrigues, "Geographic routing in random duty-cycled wireless multimedia sensor networks," in *Proc. IEEE Globecom Workshops*, Miami, FL, USA, Dec. 2010, pp. 230–234.

[5] H. Zhang and H. Shen, "Energy-efficient beaconless geographic routing in wireless sensor networks," *IEEE Trans. Parallel Distrib. Syst.*, vol. 21, no. 6, pp. 881–896, Jun. 2010.

[6] B. Karp and H. T. Kung, "GPSR: Greedy perimeter stateless routing for wireless networks," in *Proc. ACM MobiCom*, Boston, MA, USA, Aug. 2000, pp. 243–254.

[7] L. Shu, Y. Zhang, L. T. Yang, Y. Wang, M. Hauswirth, and N. Xiong, "TPGF: Geographic routing in wireless multimedia sensor networks," *Telecommun. Syst.*, vol. 44, nos. 1–2, pp. 79–95, Nov. 2009.

[8] G. Han, Y. Dong, H. Guo, L. Shu, and D. Wu, "Cross-layer optimized routing in wireless sensor networks with duty cycle and energy harvesting," *Wireless Commun. Mobile Comput.*, vol. 15, no. 16, pp. 1957–1981, Feb. 2014.

[9] C. Zhu, T. L. Yang, L. Shu, J. J. P. C. Rodrigues, and T. Hara, "A geographic routing oriented sleep scheduling algorithm in duty-cycled sensor networks," in *Proc. IEEE ICC*, Ottawa, ON, Canada, Jun. 2012, pp. 5473–5477.

[10] C. Zhu, L. T. Yang, L. Shu, V. C. M. Leung, J. J. P. C. Rodrigues, and L. Wang, "Sleep scheduling for geographic routing in duty-cycled mobile sensor networks," *IEEE Trans. Ind. Electron.*, vol. 61, no. 11, pp. 6346–6355, Nov. 2014.

[11] S. Nath and P. B. Gibbons, "Communicating via fireflies: Geographic routing on duty-cycled sensors," in *Proc. IEEE/ACM 6th Int. Symp. Inf. Process. Sensor Netw. (IPSN)*, Cambridge, MA, USA, Apr. 2007, pp. 440–449.

[12] C. Ma, L. Wang, J. Xu, Z. Qin, M. Zhu, and L. Shu, "A geographic routing algorithm in duty-cycled sensor networks with mobile sinks," in *Proc. 7th Int. Conf. Mobile Ad-Hoc Sensor Netw. (MSN)*, Beijing, China, Dec. 2011, pp. 343–344.

[13] H. M. Ammari and S. K. Das, "Joint k-coverage, duty-cycling, and geographic forwarding in wireless sensor networks," in *Proc. IEEE Symp. Comput. Commun. (ISCC)*, Tunisia, North Africa, Jul. 2009, pp. 487–492.

[14] H. Takagi and L. Kleinrock, "Optimal transmission ranges for randomly distributed packet radio terminals," *IEEE Trans. Commun.*, vol. 32, no. 3, pp. 246–257, Mar. 1984.

[15] H. Frey and I. Stojmenovic, "On delivery guarantees of face and combined greedy-face routing in ad hoc and sensor networks," in *Proc. 12th Annu. Int. Conf. Mobile Comput. Netw.*, Los Angeles, CA, USA, Sep. 2006, pp. 390–401.

[16] L. Shu, Z. Yuan, T. Hara, L. Wang, and Y. Zhang, "Impacts of duty-cycle on TPGF geographical multipath routing in wireless sensor networks," in *Proc. 18th IEEE Int. Workshop Quality Service (IWQoS)*, Beijing, China, Jun. 2010, pp. 1–2.

[17] G. Zhou, T. He, S. Krishnamurthy, and J. A. Stankovic, "Models and solutions for radio irregularity in wireless sensor networks," *ACM Trans. Sensor Netw.*, vol. 2, no. 2, pp. 221–262, 2006.

[18] M. Zuniga and B. Krishnamachari, "Analyzing the transitional region in low power wireless links," in *Proc. IEEE SECON*, Santa Clara, CA, USA, Oct. 2004, pp. 517–526.

[19] M. Mukherjee, L. Shu, L. Hu, and D.-J. Deng, "Impact of radio irregularity on wireless sensor networks," in *Proc. 2nd EAI Int. Conf. Ind. Netw. Intell. Syst. (INISCOM)*, Leicester, U.K., Oct./Nov. 2016, pp. 1–5.

[20] N. Baccour, A. Koubâa, L. Mottola, M. A. Zúñiga, H. Youssef, C. A. Boano, and M. Alves, "Radio link quality estimation in wireless sensor networks: A survey," *ACM Trans. Sensor Netw.*, vol. 8, no. 4, pp. 1–33, Sep. 2012.

[21] L. Wang, W. Washington, K. Gilmore, and C. Liu, "Impact of radio irregularities on connectivity of wireless networks with log-normal shadowing," in *Proc. 11th IEEE Int. Conf. Mobile Ad-Hoc Sensor Netw. (MSN)*, Shenzhen, China, Dec. 2015, pp. 250–257.

[22] A. Cerpa, J. L. Wong, L. Kuang, M. Potkonjak, and D. Estrin, "Statistical model of lossy links in wireless sensor networks," in *Proc. IEEE IPSN*, Los Angeles, CA, USA, Apr. 2005, pp. 81–88.

[23] J. Jiang, G. Han, H. Xu, L. Shu, and Y. Zhang, "A two-hop localization scheme with radio irregularity model in wireless sensor networks," in *Proc. IEEE WCNC*, Shanghai, China, Apr. 2012, pp. 1704–1709.

MITHUN MUKHERJEE (S'10–M'16) received the B.E. degree in electronics and communication engineering from the University Institute of Technology, Burdwan University, India, in 2007, the M.E. degree in information and communication engineering from the Indian Institute of Science and Technology, Shibpur, in 2009, and the Ph.D. degree in electrical engineering from the IIT Patna, in 2015. He is currently a Specially Assigned Researcher with the Guangdong Provincial Key Laboratory of Petrochemical Equipment Fault Diagnosis, Guangdong University of Petrochemical Technology. His research interests include wireless sensor networks, wireless communications, energy harvesting, and cloud computing.

LIKUN HU is currently pursuing the M.Sc. degree with the College of Information and Computer Engineering, Northeast Forestry University, Harbin, China. His current research interests include high processing computing, wireless sensor networks, and mobile cloud computing.

NEIL BERGMANN (M'88) received the bachelor's degrees in electrical engineering, computer science, and arts from The University of Queensland, Brisbane, QLD, Australia, and the Ph.D. degree in computer science from The University of Edinburgh in 1984. He has been the Chair of the Embedded Systems with the School of Information Technology and Electrical Engineering, The University of Queensland, since 2001. His research interests are in computer systems, especially Reconfigurable Computing and Wireless Sensor Networks. His teaching interests are in machine learning, embedded systems, and computer systems. He is a Fellow of the Institution of Engineers, Australia.

LEI SHU (M'07–SM'15) is currently a Lincoln Professor with the University of Lincoln, U.K. and a Distinguished Professor with the Guangdong University of Petrochemical Technology. He is also the Executive Director of the Guangdong Provincial Key Laboratory of Petrochemical Equipment Fault Diagnosis, China. His main research field is wireless sensor networks. He has authored over 300 papers in related conferences, journals, and books in the area of sensor networks. He had been awarded the Globecom 2010 and the ICC 2013 Best Paper Award. He has served as the TPC Member of over 150 conferences, such as the ICDCS, the DCOSS, the MASS, the ICC, the Globecom, the ICCCN, the WCNC, and the ISCC. He has also served as more than 50 various co-chair for the international conferences/workshops, such as the IWCMC, the ICC, the ISCC, the ICNC, and the Chinacom, especially the Symposium Co-Chair for the IWCMC 2012 and the ICC 2012, the General Co-Chair for the Chinacom 2014, the Qshine 2015, the Collaboratecom 2017, and the Mobiquitous 2018, and the Steering and the TPC Chair for the InisCom 2015. He has been serving as the Editor-in-Chief of the *EAI Endorsed Transactions on Industrial Networks and Intelligent Systems* and an Associate Editor of the IEEE Systems Journal and the IEEE Access.

CHUNSHENG ZHU (S'12–M'16) received the B.E. degree in network engineering from the Dalian University of Technology, China, in 2010, the M.Sc. degree in computer science from St. Francis Xavier University, Canada, in 2012, and the Ph.D. degree in electrical and computer engineering from The University of British Columbia, Canada, in 2016.

He is currently a Post-Doctoral Research Fellow with the Department of Electrical and Computer Engineering, The University of British Columbia. He has authored over 70 papers published or accepted by refereed international journals/magazines, such as the IEEE Transactions on Industrial Electronics, the IEEE Transactions on Computers, the IEEE Transactions on Information Forensics and Security, the IEEE Transactions on Emerging Topics in Computing, the IEEE Systems Journal, the IEEE Access, and the *IEEE Communications Magazine* and conferences, such as the IEEE Globecom and the IEEE ICC. His current research interests mainly include wireless sensor networks, cloud computing, Internet of Things, social networks, and security.

• • •